Available at www.sciencedirect.com

ScienceDirect

journal homepage: www.elsevier.com/locate/watres

Virus inactivation by silver doped titanium dioxide nanoparticles for drinking water treatment

Michael V. Liga [a], Erika L. Bryant [b], Vicki L. Colvin [b], Qilin Li [a,*]

[a] Department of Civil and Environmental Engineering, Rice University, 6100 Main St., Houston, TX 77005, United States
[b] Department of Chemistry, Rice University, 6100 Main St., Houston, TX 77005, United States

ARTICLE INFO

Article history:
Received 16 June 2010
Received in revised form
4 September 2010
Accepted 13 September 2010
Available online 19 September 2010

Keywords:
Drinking water
Nanotechnology
Photocatalysis
Silver
Titanium dioxide
Virus

ABSTRACT

Photocatalytic inactivation of viruses and other microorganisms is a promising technology that has been increasingly utilized in recent years. In this study, photocatalytic silver doped titanium dioxide nanoparticles (nAg/TiO_2) were investigated for their capability of inactivating Bacteriophage MS2 in aqueous media. Nano-sized Ag deposits were formed on two commercial TiO_2 nanopowders using a photochemical reduction method. The MS2 inactivation kinetics of nAg/TiO_2 was compared to the base TiO_2 material and silver ions leached from the catalyst. The inactivation rate of MS2 was enhanced by more than 5 fold depending on the base TiO_2 material, and the inactivation efficiency increased with increasing silver content. The increased production of hydroxyl free radicals was found to be responsible for the enhanced viral inactivation.

1. Introduction

The removal of viruses and other pathogens from drinking water (and the environment in general) is important for the maintenance of the health and well being of society. Pathogenic viruses such as adenovirus, norovirus, rotavirus, and hepatitis A commonly occur in both surface and groundwater sources (Abbaszadegan et al., 2003; Hamza et al., 2009; Wong et al., 2009) and must be effectively inactivated to provide safe water. In the United States just between 2003 and 2005 there were four reported waterborne disease outbreaks attributed to viruses in drinking water affecting 282 people (US Centers for Disease Control and Prevention, 2006, 2008). The USEPA requires treatment systems capable of providing 4 log (99.99%) removal of viruses for all surface water sources (US Environmental Protection Agency, 2006a) and groundwater sources with a history of contamination or other deficiencies (US Environmental Protection Agency, 2006b).

Traditional chlorine disinfection, while highly effective for viral inactivation, produces harmful disinfection byproducts (DBPs) when organic compounds are present in the water. This has prompted stricter regulations concerning the acceptable levels of these compounds (US Environmental Protection Agency, 2006c). Although UV disinfection has not been found to form DBPs (Liberti et al., 2003), some viruses such as adenoviruses are highly resistant to UV disinfection (Yates et al., 2006). As a result, the USEPA has increased the UV fluence requirements for 4 log removal of viruses from 40 mJ/cm^2 to 186 mJ/cm^2 (US Environmental Protection Agency, 2006a). The new high fluence requirement significantly increases the energy demand, which translates into a higher treatment cost.

* *Corresponding author*. Tel.: +1 713 348 2046.
E-mail address: qilin.li@rice.edu (Q. Li).
0043-1354/$ – see front matter © 2010 Elsevier Ltd. All rights reserved.
doi:10.1016/j.watres.2010.09.012

The employment of a highly efficient photocatalyst for advanced oxidation could potentially enable effective virus inactivation in drinking water as chlorine can while limiting the formation of DBPs (Liu et al., 2008). It would also require less energy than UV disinfection. Therefore, photocatalytic oxidation is being actively researched as an alternative water disinfection method (Lydakis-Simantiris et al., 2010; Sordo et al., 2010). A highly efficient photocatalyst could also be utilized for air treatment or as an antimicrobial coating.

1.1. *Titanium dioxide photocatalysis*

Titanium dioxide is an attractive photocatalyst for water treatment as it is resistant to corrosion and non toxic when ingested (Kaneko and Okura, 2002). The basic mechanism of TiO_2 photoactivation and reactive oxygen species (ROS) generation is well known (Hoffmann et al., 1995).

There are currently a few commercial treatment systems that utilize TiO_2 photocatalysis (e.g. Wallenius AOT®, Purifics®). However their usage is not wide spread. One major reason for the limited application is the slow reaction kinetics as a consequence of charge recombination, which consumes the activated electrons and holes.

The antibacterial properties of TiO_2 have been well documented (Wei et al., 1994; Watts et al., 1995; Kikuchi et al., 1997; Cho et al., 2005; Benabbou et al., 2007; Page et al., 2007) and are attributed to the generation of ROS, especially hydroxyl free radicals ($HO^{\bullet}$) and hydrogen peroxide (H_2O_2) (Kikuchi et al., 1997). While fewer studies have investigated the antiviral properties of TiO_2, its potential for inactivating viruses has been demonstrated (Watts et al., 1995; Belháčová et al., 1999; Koizumi and Taya, 2002; Cho et al., 2005). However, the inactivation rates obtained in most of these studies were extremely low. For example, Cho et al. (2005) demonstrated only ~1 log removal of MS2 after 2 h of irradiation using P25 TiO_2 suspended at 1 g/L. The inactivation kinetics needs to be greatly improved in order to provide efficient drinking water disinfection.

Metal doping has been used to enhance TiO_2 photocatalysis by trapping excited electrons to prevent charge recombination (Mu et al., 1989; Choi et al., 1994; Haick and Paz, 2003; Iliev et al., 2006). Electron trapping can occur if the dopant has a lower Fermi level than the excited electron. Several metals including Fe, Mo, Ru, Os, Re, V, Rh, Au, Pt, and Ag have been shown to enhance TiO_2 performance. Silver in particular has been shown to enhance the photocatalytic efficiency of TiO_2 for both organic contaminant degradation and bacterial inactivation (Kondo and Jardim, 1991; Vamathevan et al., 2002; Zhang et al., 2003; Xin et al., 2005; Page et al., 2007; Seery et al., 2007). Tran et al. (2006) showed selective enhancement by silver, which increased degradation rates for short chain carboxylic acids but not for alcohols or aromatics. Silver coatings above the optimum amount can also decrease the photocatalytic activity (Sclafani et al., 1991; Sung-Suh et al., 2004). However, there is limited information on its impact on the antiviral capabilities of TiO_2 (Kim et al., 2006). In addition to facilitating charge separation, silver is thought to enhance TiO_2 photocatalysis by directly interacting with microorganisms and providing more surface area for adsorption (Sclafani et al., 1997; Sung-Suh et al., 2004), although Vamathevan et al. (2002) found no increase in BET surface area after silver doping. Silver ions and nanoparticles have been shown to have antimicrobial properties themselves through a variety of mechanisms (Feng et al., 2000; Elechiguerra et al., 2005; Morones et al., 2005), which could also aid in bacterial or viral inactivation.

Utilizing silver in conjunction with TiO_2 photocatalysis could potentially allow several different inactivation mechanisms to work in concert. Therefore, it is possible that a synergism occurs between silver and TiO_2 when silver doped titanium dioxide is used for inactivating microorganisms under UV radiation. The study reported here demonstrated that silver doping TiO_2 greatly enhanced the photocatalytic inactivation of viruses primarily by increasing $HO^{\bullet}$ production in addition to slightly increasing virus adsorption.

2. Materials and methods

2.1. *Synthesis and characterization of nano-silver doped TiO_2 (nAg/TiO_2)*

nAg/TiO_2 was prepared by depositing nano-sized silver islands via photochemical reduction of silver nitrate (Alfa Aesar) onto two commercially available TiO_2: Aeroxide TiO_2 P 25 (denoted hereafter P25 TiO_2, Degussa) and Anatase TiO_2 (denoted hereafter $AATiO_2$, Alfa Aesar; CAS: 1317-70-0). A solution containing oxalic acid (Sigma–Aldrich, anhydrous 99%) as a sacrificial electron donor, TiO_2, and silver nitrate (Sigma–Aldrich, 99.9999%) was stirred for 2 h at pH 1 under ambient light at room temperature while purged with nitrogen gas. The solution was then irradiated with a germicidal UV lamp for one day and the product purified by washing with excessive water four times (Iliev et al., 2006). The concentration of silver nitrate used in the reaction solution was varied to achieve 4, 8, and 10 wt.%; oxalic acid was added at a 25:1 acid to silver molar ratio. The $AATiO_2$ was doped using 10% $AgNO_3$ in solution. The doped particles were then dried and stored under vacuum in dark.

Samples were prepared for TEM and XPS analysis by applying a drop of a $nAgTiO_2$ suspension to a Silicon Monoxide/Formvar grid (Ted Pella; 01829) or a silicon wafer coated with gold (~68 nm). The grid was then used to analyze the sample in a JEOL 2100 field emission gun transmission electron microscope (JEM 2100F TEM) at 200 KV. The silicon wafer was used for x-ray photoelectron spectroscope (PHI Quantera XPS).

The actual silver content of the nAg/TiO_2 nanoparticles was determined by acid digestion and subsequent analysis of silver concentration using inductively coupled plasma-optical emission spectroscopy (ICP–OES, PerkinElmer Optima 4300 DV). Aliquots of 0.01 g nAg/TiO_2 nanoparticles were mixed with 5 mL of 50% HNO_3, briefly bath sonicated, refluxed for 4 h and diluted to 50 mL with ultrapure water. The resulting suspensions were centrifuged and the supernatants filtered through a 0.22 μm-pore-size syringe filter. The filtrates were then analyzed by ICP–OES to determine the silver concentration.

2.2. Model virus

Bacteriophage MS2 (ATCC 15597-B1) was used as a model virus in this study due to its similarity to many waterborne pathogenic viruses (Koizumi and Taya, 2002; Mackey et al., 2002; Butkus et al., 2004) and the simplicity of its propagation and enumeration. MS2 has been found to be comparable or more resistant to chlorine and chloramines than Hepatitis A virus (Sobsey et al., 1988) and Poliovirus (Tree et al., 2003), and more resistant to UV disinfection than other bacteriophages (Sommer et al., 2001). Hence, using MS2 as a virus surrogate provides conservative assessment on treatment efficiency.

The virus stock solution used in the disinfection procedures was obtained by infecting an incubation of the E. coli host (ATCC 15597) with a liquid MS2 suspension. The mixture was mixed with a molten LB–Lennox (Fisher) medium containing 0.7% Bacto™ agar (Difco Laboratories) and poured over a Petri dish containing solid LB–Lennox media. After incubating overnight at 37 °C, sterile 0.1 M bicarbonate (Fisher) buffer was added to the plate which was gently rocked for 3 h. The solution was withdrawn from the plate, centrifuged, and the supernatant filtered through a 0.22 μM-pore-size PES syringe filter (Cho et al., 2005). The virus suspension contained $\sim 7 \times 10^9$ plaque forming units per milliliter (PFU/mL) and was stored at 4 °C before use.

MS2 samples were enumerated according to the double agar layer method (Adams, 1959). Samples were analyzed either immediately or stored at 4 °C in dark and analyzed within 24 h. No change in viral titers was found within 24 h of storage in the presence or absence of the nanomaterials. To determine if the presence of nanoparticles interfered with virus enumeration, parallel samples containing nanoparticles were enumerated directly or after centrifugation at 10,900 × *g* for 15 min to remove the nanoparticles. No significant difference was found between the two methods. Therefore, all data reported hereafter were obtained from direct enumeration of the samples without removing the nanoparticles. Control tests consisted of enumerating buffer solution to ensure that viral contamination was not present in any of the reagents.

2.3. Virus inactivation experiments

All materials that came in contact with the virus solutions, media, and reagents were sterilized by autoclaving, filtering, or purchased sterile. Nanoparticle suspensions were freshly prepared in ultrapure water and were bath sonicated for 30–45 min to ensure good dispersion before each experiment. Particle size and zeta potential of each suspension was analyzed by dynamic light scattering (DLS) using a Zen 3600 Zetasizer (Malvern Instruments, Worcestershire, UK) to determine if differences in particle size and thus surface area were responsible for any observed differences in viral inactivation.

2.3.1. Dark inactivation of viruses

Dark inactivation of viruses was assessed using undoped P25 TiO_2 and nAg/TiO_2 synthesized with P25 and 10 wt.% $AgNO_3$. A suspension of $\sim 7 \times 10^7$ PFU/mL MS2 was made in ultrapure water to which sonicated nAg/TiO_2 or P25 TiO_2 nanoparticles were added. The suspension was then stirred for up to 10 min in the dark, and sampled at different times for virus enumeration. The virus/nanoparticle mixtures were subsequently kept in dark at 4 °C for 24 h before enumerated again. The effect of leached silver was investigated by removing the catalyst particles from suspension after sonication by centrifugation and filtration. The resulting solution was added to an MS2 suspension, which was sampled periodically for the active MS2 titer.

2.3.2. Photocatalytic virus inactivation

The photocatalytic viral inactivation experiments were carried out in a pre-stabilized Luzchem LZC-4V photoreactor (Luzchem Research, Inc., Ottawa, ON Canada) fitted with four 8 W UV-A (315–400 nm) lamps with peak emission at 350 nm (Hitachi). The total light intensity used in all experiments was 2.5 mW/cm^2 as determined by a UV radiometer (Control Company, Friendswood, TX) with a NIST traceable 350 nm photosensor.

Reactions were housed in sealed 25 mL Pyrex Erlenmeyer flasks. Sterile ultrapure water was combined with the MS2 stock solution and catalyst suspensions or leached Ag^+ solutions to achieve a final concentration of $\sim 7 \times 10^7$ PFU/mL MS2 and 100 mg/L TiO_2 or nAg/TiO_2. The volume of leached Ag^+ solution added was the same as that used with particles in suspension. The mixture was stirred for 1 min in the dark, after which a sample was taken representing the initial virus concentration after adsorption. The reaction flask was then placed in the reactor and 1 mL samples were taken at 30 s intervals. All samples were immediately enumerated or covered and refrigerated at 4 °C to prevent further inactivation while waiting to be processed.

To investigate the role of HO• in MS2 inactivation, reactions were carried out in the presence of two HO• scavengers, methanol (99.9%, Fisher spectranalyzed) or *tert*-butanol (Fisher, ACS Certified) at concentrations from 30 to 400 mM. Control experiments were performed by mixing MS2 in the corresponding alcohol solution for 10 min to account for any inactivation due to the alcohol. Samples were immediately diluted into 0.1 M bicarbonate buffer.

3. Results and discussion

3.1. nAg/TiO_2 characterization

The color of the dried nAg/TiO_2 nanoparticles varied from light brown to reddish brown. The degree of surface oxidation of the silver is likely responsible for the differences in color.

3.1.1. Silver content

The amount of silver captured by the TiO_2 varied with both the $AgNO_3$ concentration and the base TiO_2 material used. The P25 TiO_2 based nAg/TiO_2 made with 10, 8, and 4 wt.% $AgNO_3$ had final Ag contents of 5.95, 4.36, and 2.46 wt.%. The AATiO_2 based nAg/TiO_2 made with 10 wt.% $AgNO_3$ had a final Ag content of 3.94 wt.%. The nAg/TiO_2 materials are hereafter designated by the final nAg content and base TiO_2 material (e.g. 5.95%nAg/P25TiO_2). Silver deposition was more efficient at higher $AgNO_3$ concentrations. Deposition onto P25 was notably greater than that on the AATiO_2: 90% of the Ag added

was coated onto P25 while only 59% onto the $AATiO_2$ when 10% $AgNO_3$ was applied. The lower doping efficiency of $AATiO_2$ is attributed to its limited photoactivity.

3.1.2. *TEM and XPS analyses*

Fig. 1 presents representative TEM images of the Ag doped and undoped P25 samples. Silver islands of ~2–4 nm in diameter were found on the TiO_2 nanoparticles (~10–50 nm), although they were not apparent on all crystallites. No silver deposits were observed on any TiO_2 particles not treated with silver.

XPS analyses showed similar results for all samples. Fig. 2 presents the XPS spectra for the 5.95%nAg/P25TiO_2 as an example. O 1s spectra (e.g., Fig. 2a) of all samples showed a major peak with a broad shoulder in the area for metal oxides (528–531 eV). The presence of the shoulder indicates the presence of multiple metal oxides, i.e., titanium dioxide and silver oxide. The Ag 3d spectra (e.g., Fig. 2b) confirm the presence of silver oxide (peak range 367.3–368.0). This may be due to silver adsorbing on the TiO_2 surface at oxygen sites or the oxidation of the surface of the deposited silver.

3.1.3. *Dispersed particle size*

Mean hydrodynamic diameters of all photocatalyst suspensions in ultrapure water are presented in Fig. 3. The sizes of P25 TiO_2, $AATiO_2$, and 3.94%nAg/$AATiO_2$ stayed constant for at least 25 min, suggesting that these suspensions were stable during the virus inactivation experiments (~5 min). All the P25 based nAg/TiO_2 materials, however, formed large aggregates and settled out gradually. The aggregation of the silver doped samples was consistent with the measured changes in zeta potential: −9.1–−9.3 mV versus −38.7 mV for P25. The sizes presented in Fig. 3 for these materials are the average of data obtained in the first 5 min concurrent with the inactivation procedure.

3.2. *MS2 dark inactivation*

Inactivation and removal of MS2 by the photocatalysts in dark (referred to as dark inactivation hereafter) is attributed to adsorption to the photocatalyst particles and inactivation by Ag^+ released from nAg/TiO_2. Fig. 4 shows the total dark

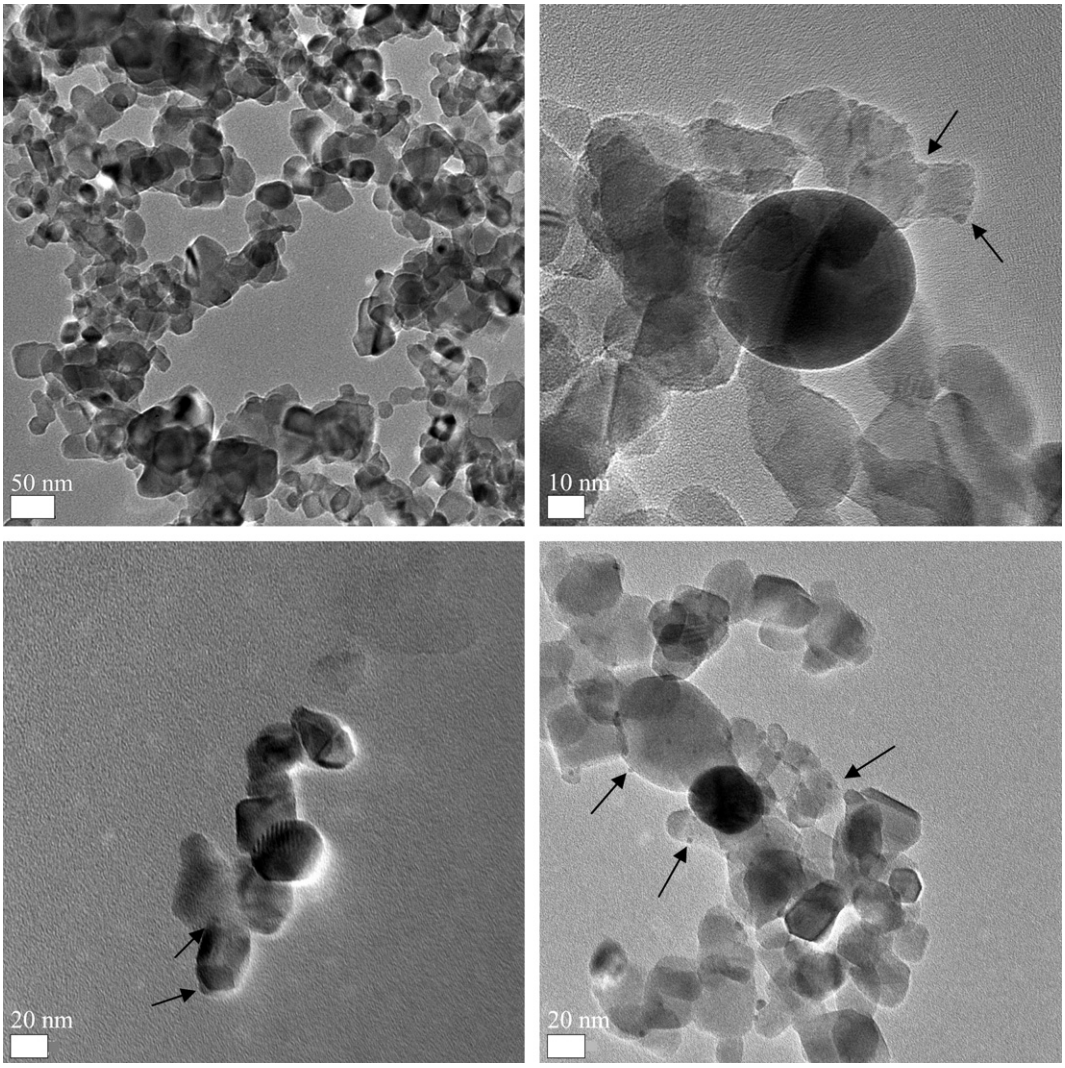

Fig. 1 – TEM images of nAg/P25TiO_2 with silver particles (~2–4 nm dia.) indicated by arrows. Silver particles are visible on all doped samples, although they are not apparent on all TiO_2 crystallites (10–50 nm dia.). Top left undoped P25 (50 nm scale), top right 5.95% Ag (10 nm scale), bottom left 4.36% Ag (20 nm scale), bottom right 2.46% Ag (20 nm scale).

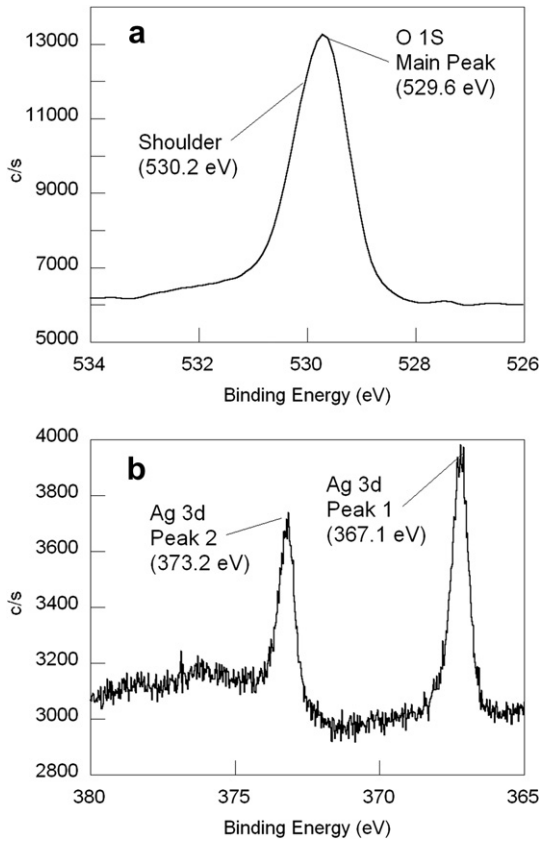

Fig. 2 – Typical X-ray photoelectron spectra of (a) O 1s, which reveals the presence of multiple metal oxides through the observed peak shoulder and (b) Ag 3d, with peak between 367.3 and 368 eV which corresponds to silver oxide. Spectra shown for 5.95%nAg/P25TiO$_2$.

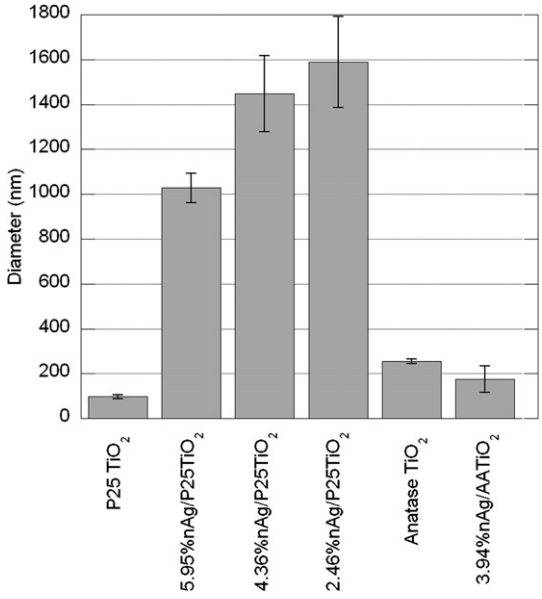

Fig. 3 – Dispersed particle diameters of nanoparticles used for virus inactivation as measured by DLS. Silver doping P25 TiO$_2$ was found to decrease the stability of the suspended particles, resulting in the observed aggregation.

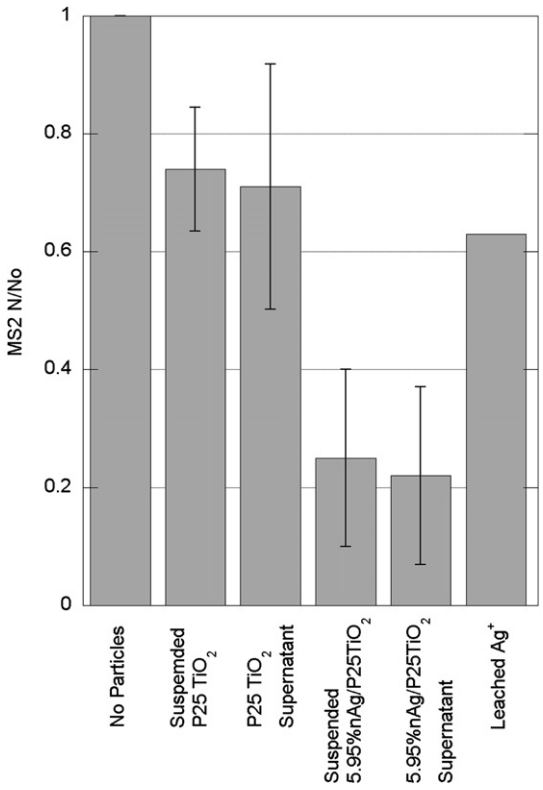

Fig. 4 – Removal of MS2 by P25 TiO$_2$, 5.95%nAg/P25TiO$_2$, and leached Ag$^+$ from 5.95%nAg/P25TiO$_2$ after 10 min of contact in dark. TiO$_2$ and nAg/TiO$_2$ samples were enumerated both with particles in suspension and after their removal by centrifugation (data marked "supernatant") to determine if adsorbed viruses remained infective. The limited difference in virus titers between solutions with particles suspended and removed suggests that MS2 is inactivated upon adsorption to the catalysts. After accounting for the effect of leached Ag$^+$, the 5.95% nAg/P25TiO$_2$ removed 38% (75–37%) MS2 by adsorption as compared to only 26% by P25 TiO$_2$.

removal after 10 min of exposure to P25 and 5.95%nAg/P25TiO$_2$. Leached Ag$^+$ was responsible for 37% (0.2 log) MS2 inactivation, with most inactivation occurring during the first 1 min of exposure. When enumerated with catalyst particles in suspension, a total of 75% (0.6 log) removal was observed with 5.95%nAg/P25TiO$_2$. After accounting for the effect of leached Ag$^+$ (37% removal), the 5.95%nAg/TiO$_2$ removed 38% (0.2 log) of the MS2 by adsorption, 12% more than that adsorbed by undoped P25, which inactivated 26% (0.13 log) of the MS2. The majority of dark inactivation occurred during the first minute of exposure. Therefore, the MS2 concentration measured after 1 min of dark contact in each photocatalytic inactivation experiment was used as the initial concentration for analysis of the photocatalytic inactivation data.

The increased adsorptive removal by nAg/TiO$_2$ may be explained by interactions of viral surface amino acids with silver. Silver has a high affinity for sulfur moieties, and there are 183 cysteine residues exposed on the MS2 capsid surface (Jou et al., 1972; Nolf et al., 1977; Penrod et al., 1996). Carboxyl

groups on the amino acids are also known to interact with silver (Stewart and Fredericks, 1999). The minimum difference between virus titers with nanoparticles in suspension and nanoparticle free centrifuge supernatant (Fig. 4) suggests that adsorption of MS2 to the nAg/TiO_2 or undoped TiO_2 surface either inactivates these viruses or sterically inhibits access of the MS2 A protein to the *E. coli* pili, where infection occurs. The limited additional removal observed after centrifugation of samples is attributed to the interception of MS2 by the catalyst particles during centrifugation.

The mixtures of the MS2 and the P25 TiO_2 or 5.95%nAg/P25TiO_2 were further kept in dark at 4 °C for 24 h and re-enumerated to assess the potential dark inactivation of stored samples. Negligible change in virus titer was observed during the 24 h period for either materials (data not shown), suggesting that further inactivation was absent in dark.

3.3. *Photocatalytic MS2 inactivation*

The inactivation of MS2 by the different nanomaterials and UV-A alone is shown in Fig. 5. The plain P25 TiO_2 achieved 1.6 log inactivation of MS2 in 2 min while UV-A irradiation alone showed negligible MS2 removal within the same time period (Fig. 5a), showing that the inactivation in the presence of P25 TiO_2 is attributed to photocatalytic oxidation. Silver doping significantly enhanced MS2 inactivation by P25 TiO_2 and the inactivation rate increased with silver content. The enhanced inactivation was also observed with the Ag doped AATiO_2 (Fig. 5b), even though AATiO_2 showed minimum inactivation.

The photocatalytic inactivation kinetics data could be described by the Chick–Watson model (Equation (1)), where k is the rate constant (s^{-1}) and N_0 and N are the titer of active viruses at time zero and t. Here, the virus titer after dark adsorption equilibrium was used as N_0.

$$\log\left(\frac{N}{N_0}\right) = -kt \quad (1)$$

The inactivation rate constants obtained from fitting the kinetics data with the Chick–Watson model are shown in Table 1. The silver doping increased the reaction rate constant by up to 584% as compared to the base TiO_2. The inactivation rate was found to increase with the silver content on P25 TiO_2, with rate constants of 0.089, 0.035, 0.017 and 0.013 s^{-1}, for the materials with 5.95, 4.36, 2.46 and 0% silver, respectively. The inactivation rate constant for 3.94%nAg/AATiO_2 (0.024 s^{-1}) showed a 5 fold increase from the plain AATiO_2 (0.004 s^{-1}); it also outperformed P25 TiO_2 and 2.46%nAg/P25TiO_2, even though the P25 TiO_2 inactivated MS2 ~3.2 times faster than the AATiO_2. While silver was found to be beneficial when doped onto P25 TiO_2, the increased aggregate size may have offset some enhancement in photoactivity. Also shown in Table 1 is the time required for each nanomaterial to achieve 4 log removal of MS2. With 5.95 wt.% nAg loading on P25, 4 log removal of MS2 could be obtained in 45 s, making it feasible to achieve virus removal from drinking water using a small photoreactor or to improve removal of UV resistant viruses of existing UV reactors.

Experiments using solutions containing leached Ag^+ resulted in no notable photocatalytic inactivation. These results suggest that the enhanced inactivation was due to the increase in the photocatalytic activity of TiO_2 instead of the antimicrobial property of nAg. Two mechanisms may be responsible for such enhancement: increased MS2 adsorption and greater ROS generation. MS2 inactivation has been shown to be directly proportional to the amount adsorbed to the TiO_2 surface (Koizumi and Taya, 2002). Increased adsorption as demonstrated in Fig. 4 may enhance the inactivation rate by placing the virus in close proximity to newly generated HO•

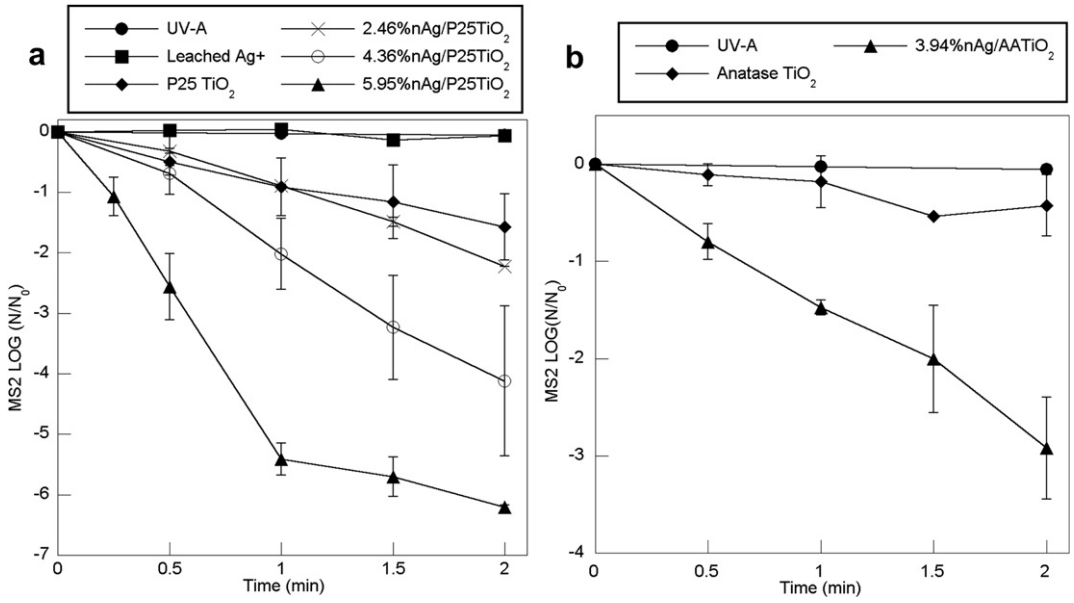

Fig. 5 – MS2 Inactivation by (a) UV-A alone and Ag^+, P25 TiO_2, 2.46%nAg/P25TiO_2, 4.36%nAg/P25TiO_2, and 5.95%nAg/P25TiO_2 under UV-A irradiation, and by (b) UV-A alone and, AATiO_2, 3.94%nAg/AATiO_2 under UV-A irradiation. The inactivation rate was found to increase along with the silver content on P25 TiO_2 up to the maximum amount tested (5.95%). 3.94% nAg on anatase TiO_2 also dramatically increased the inactivation rate.

Table 1 – Actual silver contents on nAg/TiO_2 particles and first order rate constants for MS2 inactivation.

Material	Rate Constant (s^{-1})	R^2	Time Required to Achieve 4 Log Removal (min)[a]
P25 TiO_2	0.013	0.91	5.1
2.46%nAg/P25TiO_2	0.017	0.99	3.9
4.36%nAg/P25TiO_2	0.035	0.97	1.9
5.95%nAg/P25TiO_2	0.089[b]	0.99	0.75
AATiO_2	0.004	0.98	16.7
3.94%nAg/AATiO_2	0.024	0.99	2.8

a Times greater than 2 min obtained by projecting kinetic data.
b Rate for first 60 s of inactivation.

(both surface bound and bulk) and may increase direct hole oxidation. In addition, silver doping has been proposed to facilitate charge separation in TiO_2 resulting in more efficient ROS generation and consequently greater MS2 inactivation.

MS2 inactivation by 5.95%nAg/P25TiO_2 shows a tailing effect after 60 s (5.4 log removal), when the inactivation rate constant decreased from 0.089 to 0.013. This was not observed when MS2 was inactivated by the other materials. This is likely due to the presence of the large number of inactivated viruses and their remnants, which compete with infective viruses for adsorption sites and ROS, since 99.9996% of the MS2 had been inactivated after 60 s.

3.3.1. *Effects of HO• scavengers*

As discussed above, one potential mechanism for the enhanced virus inactivation of nAg/TiO_2 is higher HO• production rate. To test this mechanism, methanol and *tert*-butanol were employed to elucidate the role of Ag doping in HO• production and MS2 inactivation. Alcohols, especially methanol and *t*-butanol, are known HO• scavengers. Methanol was reported to scavenge both surface bound and bulk HO•, as well as holes (Cho et al., 2005). While *t*-butanol has been shown to competitively adsorb to TiO_2 (Sun and Pignatello, 1995), research has demonstrated that it does not scavenge all surface bound HO• (Kim and Choi, 2002). Using methanol and *t*-butanol as HO• scavengers, Cho et al. (2005) showed that bulk HO• was responsible for the inactivation of MS2 by TiO_2. Singlet oxygen and superoxide anion were also found to

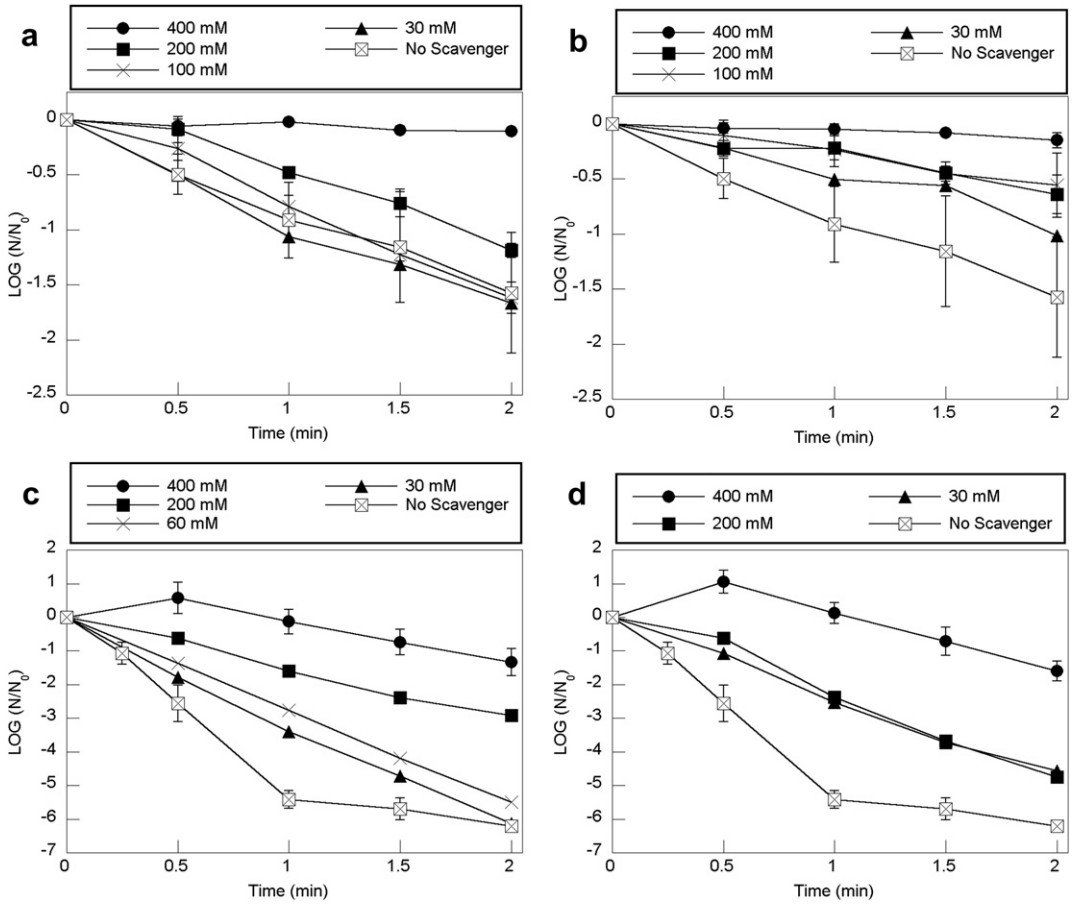

Fig. 6 – MS2 inactivation in the presence of HO• scavengers methanol and *t*-butanol. (a) P25 TiO_2 with methanol; (b) P25 TiO_2 with *t*-butanol; (c) 5.95%nAg/P25TiO_2 with methanol; (d) 5.95%nAg/P25TiO_2 with *t*-BuOH. The inactivation rate was found to decrease in a concentration dependent manner when either alcohol was applied. When present at 400 mM, both alcohols completely stopped MS2 inactivation by P25 TiO_2 while inactivation still occurred by 5.95%nAg/P25TiO_2, but to a much lesser degree than the case when no HO• scavenger is applied. Dark inactivation of MS2 by 5.95%nAg/P25TiO_2 was enhanced when either alcohol was present at 400 mM, but the effect was reversed after 30 s of irradiation corresponding to the apparent initial rise in active virus titer.

inactivate MS2 in a study using fullerol as the photocatalyst (Badireddy et al., 2007).

Experiments were performed using P25 TiO_2 (Fig. 6a,b) and 5.95%nAg/P25TiO_2 (Fig. 6c,d) at different methanol or *t*-butanol concentrations. Both methanol and *t*-butanol completely stopped inactivation of MS2 by the plain P25 TiO_2 at 400 mM and considerably slowed the reaction at 200 mM. P25 TiO_2 showed higher sensitivity to *t*-butanol, as 30 and 100 mM *t*-butanol both decreased the inactivation rate while the same concentrations of methanol had no effect. Control experiments using methanol or *t*-butanol in the absence of any photocatalyst did not show any decrease in virus titer for methanol or *t*-butanol concentrations up to 400 mM. These results suggest that HO• is primarily responsible for MS2 inactivation by P25 TiO_2. Although singlet oxygen and superoxide anions are also produced by TiO_2 (Hoffmann et al., 1995), they did not seem to cause notable MS2 inactivation in our study. Because there was no significant difference in reaction rates when either methanol or *t*-butanol was used at 400 mM and the inactivation rate was more sensitive to low *t*-butanol concentrations, the data suggests that bulk HO• plays a more important role than surface bound HO• in MS2 inactivation. This observation agrees with the conclusion by Cho et al. (2005).

Both alcohols also reduced the inactivation rate of MS2 by 5.95%nAg/P25TiO_2, but to a much less extent. With 400 mM methanol or *t*-butanol, 1.3 and 1.6 log of MS2 inactivation was achieved, respectively, suggesting that silver doping increases HO• production and consequently MS2 inactivation. When nAg/TiO_2 was used with 400 mM of either alcohol, the amount of viruses removed by dark stirring was greater than that observed without added alcohol (90–98%, data not shown). The active virus titer increased after 30 s of irradiation compared to that before UV exposure. Since the depression of initial virus concentration was not observed with undoped P25 TiO_2, this effect is attributed to the interaction of the alcohol with the silver and the subsequent changes in viral adsorption capacity. Any increased adsorption of alcohol to silver/silver oxide as compared to TiO_2 could change the electrostatic and/or hydrophilic properties of the catalyst, resulting in changes to its adsorptive capacity. From 30 s to 2 min, the MS2 was slowly inactivated. The inactivation rate by nAg/TiO_2 was observed to be influenced by both alcohols in a concentration dependent manner, confirming the role of HO• in MS inactivation.

4. Conclusion

This study demonstrated that silver doping TiO_2 nanoparticles is an effective way to increase TiO_2 photocatalytic activity for virus inactivation. Silver doping enhances photocatalytic inactivation of viruses primarily by increasing HO• production, although increased virus adsorption to silver sites and leaching of antimicrobial Ag^+ also contribute to virus removal. The fast virus inactivation kinetics of the nAg/TiO_2 materials demonstrated in our study suggest that effective virus inactivation can be achieved using a small photoreactor and photocatalytic disinfection of drinking water at both point of use and municipality scales could be a potential application of the nAg/TiO_2 materials. Further research is needed to address issues such as photocatalyst fouling, impact of water quality, loss of silver, and need for catalyst regeneration to ensure the sustainability of the technology. Very importantly, the retention of the nAg/TiO_2 materials in the treatment system is critical. This can be achieved by using a hybrid photoreactor/membrane system, where the photocatalyst is retained by a membrane unit down-stream of the photoreactor and recirculated, or by applying the photocatalyst as a coating on surfaces inside a photoreactor. Because UV-A is a significant component of the solar irradiation that reaches earth surface, coating transparent piping or shallow open channels with the photocatalyst at sunny locations could also be a low-cost solution to drinking water disinfection. Ag/TiO_2 may also be activated by visible light through the silver surface plasmon resonance, however it is not clear how the catalyst will behave under both UV and visible radiation (Sung-Suh et al., 2004; Seery et al., 2007).

Acknowledgements

This work was supported by the Center for Biological and Environmental Nanotechnology at Rice University (NSF Award EEC-0647452). Laboratory work was assisted by Zoltan Krudy.

REFERENCES

Abbaszadegan, M., Lechevallier, M., Gerba, C., 2003. Occurrence of viruses in US groundwaters. Journal-American Water Works Association 95 (9), 107–120.

Adams, M.H., 1959. Bacteriophages. Interscience Publishers, Inc., New York.

Badireddy, A.R., Hotze, E.M., Chellam, S., Alvarez, P., Wiesner, M.R., 2007. Inactivation of bacteriophages via photosensitization of fullerol nanoparticles. Environmental Science & Technology 41 (18), 6627–6632.

Belháčová, L., Krysa, J., Geryk, J., Jerkovsky, J., 1999. Inactivation of microorganisms in a flow-through photoreactor with an immobilized TiO_2 layer. Journal of Chemical Technology and Biotechnology 74, 149–154.

Benabbou, A.K., Derriche, Z., Felix, C., Lejeune, P., Guillard, C., 2007. Photocatalytic inactivation of Escherichia coli – effect of concentration of TiO_2 and microorganism, nature, and intensity of UV irradiation. Applied Catalysis B-Environmental 76 (3–4), 257–263.

Butkus, M.A., Labare, M.P., Starke, J.A., Moon, K., Talbot, M., 2004. Use of aqueous silver to enhance inactivation of coliphage MS-2 by UV disinfection. Applied and Environmental Microbiology 70 (5), 2848–2853.

Cho, M., Chung, H., Yoon, J., 2005. Different inactivation behaviors of MS-2 phage and Escherichia coli in TiO_2 photocatalytic disinfection. Applied and Environmental Microbiology 71 (1), 270–275.

Choi, W., Termin, A., Hoffmann, M., 1994. The role of metal ion dopants in quantum size TiO_2: correlation between photoreactivity and charge carrier recombination dynamics. Journal of Physical Chemistry 98, 13669–13679.

Elechiguerra, J.L., Burt, J.L., Morones, J.R., Camacho-Bragado, A., Gao, X., Lara, H.H., Yacaman, M.J., 2005. Interaction of silver nanoparticles with HIV-1. Journal of Nanobiotechnology 3 (6).

Feng, Q.L., Wu, J., Chen, G.Q., Cui, F.Z., Kim, T.N., Kim, J.O., 2000. A mechanistic study of the antibacterial effect of silver ions on Escherichia coli and Staphylococcus aureus. Journal of Biomedical Materials Research 52 (4), 662–668.

Haick, H., Paz, Y., 2003. Long-range effects of noble metals on the photocatalytic properties of titanium dioxide. Journal of Physical Chemistry B 107 (10), 2319–2326.

Hamza, I.A., Jurzik, L., Stang, A., Sure, K., Uberla, K., Wilhelm, M., 2009. Detection of human viruses in rivers of a densly-populated area in Germany using a virus adsorption elution method optimized for PCR analyses. Water Research 43 (10), 2657–2668.

Hoffmann, M.R., Martin, S.T., Choi, W., Bahnemann, D.W., 1995. Environmental application of semiconductor photocatalysis. Chemical Reviews 95 (1), 69–95.

Iliev, V., Tomova, D., Bilyarska, L., Eliyas, A., Petrov, L., 2006. Photocatalytic properties of TiO_2 modified with platinum and silver nanoparticles in the degradation of oxalic acid in aqueous solution. Applied Catalysis B-Environmental 63 (3–4), 266–271.

Jou, W.M., Ysebaert, M., Fiers, W., Haegeman, G., 1972. Nucleotide sequence of gene coding for bacteriophage MS2 coat protein. Nature 237 (5350), 82–88.

Kaneko, M., Okura, I.E. (Eds.), 2002. Photocatalysis: Science and Technology. Springer, New York.

Kikuchi, Y., Sunada, K., Iyoda, T., Hashimoto, K., Fujishima, A., 1997. Photocatalytic bactericidal effect of TiO_2 thin films: dynamic view of the active oxygen species responsible for the effect. Journal of Photochemistry and Photobiology A: Chemistry 106, 51–56.

Kim, J.-P., Cho, I.-H., Kim, I.-T., Kim, C.-U., Heo, N.H., Suh, S.-H., 2006. Manufacturing of anti-viral inorganic materials from colloidal silver and titanium dioxide. Revue Romaine de Chimie 51 (11), 1121–1129.

Kim, S., Choi, W., 2002. Kinetics and mechanisms of photocatalytic degradation of $(CH3)_nNH_{4-n}^{+}$ $(0 \leq n \leq 4)$ in TiO_2 suspension: the role of OH radicals. Environmental Science & Technology 36 (9), 2019–2025.

Koizumi, Y., Taya, M., 2002. Kinetic evaluation of biocidal activity of titanium dioxide against phage MS2 considering interaction between the phage and photocatalyst particles. Biochemical Engineering Journal 12 (2), 107–116.

Kondo, M.M., Jardim, W.F., 1991. Photodegradation of chloroform and urea using Ag-loaded titanium dioxide as catalyst. Water Research 25 (7), 823–827.

Liberti, L., Notarnicola, M., Petruzzelli, D., 2003. Advanced treatment for municipal wastewater reuse in agriculture. UV disinfection: parasite removal and by-product formation. Desalination 152 (1–3), 315–324.

Liu, S., Lim, M., Fabris, R., Chow, C., Drikas, M., Amal, R., 2008. TiO_2 photocatalysis of natural organic matter in surface water: impact on trihalomethane and haloacetic acid formation potential. Environmental Science & Technology 42 (16), 6218–6223.

Lydakis-Simantiris, N., Riga, D., Katsivela, E., Mantzavinos, D., Xekoukoulotakis, N.P., 2010. Disinfection of spring water and secondary treated municipal wastewater by TiO_2 photocatalysis. Desalination 250 (1), 351–355.

Mackey, E.D., Hargy, T.M., Wright, H.B., Malley, J.P., Cushing, R.S., 2002. Comparing cryptosporidium and MS2 bioassays – implications for UV reactor validation. Journal-American Water Works Association 94 (2), 62–69.

Morones, J.R., Elechiguerra, J.L., Camacho, A., Holt, K., Kouri, J.B., Ramirez, J.T., Yacaman, M.J., 2005. The bactericidal effect of silver nanoparticles. Nanotechnology 16, 2346–2353.

Mu, W., Herrmann, J.M., Pichat, P., 1989. Room-temperature photocatalytic oxidation of liquid cyclohexane over neat and modified TiO_2. Catalysis Letters 3 (1), 73–84.

Nolf, F.A., Vandekerckhove, J.S., Lenaerts, A.K., Vanmontagu, M.C., 1977. Sequence of A-protein of coliphage-MS2. 1. Isolation of A-protein, determination of NH_2-terminal and COOH-terminal sequences, isolation and amino-acid sequence of tryptic peptides. Journal of Biological Chemistry 252 (21), 7752–7760.

Page, K., Palgrave, R.G., Parkin, I.P., Wilson, M., Savin, S.L.P., Chadwick, A.V., 2007. Titania and silver–titania composite films on glass-potent antimicrobial coatings. Journal of Materials Chemistry 17 (1), 95–104.

Penrod, S.L., Olson, T.M., Grant, S.B., 1996. Deposition kinetics of two viruses in packed beds of quartz granular media. Langmuir 12 (23), 5576–5587.

Sclafani, A., Mozzanega, M.N., Pichat, P., 1991. Effect of silver deposits on the photocatalytic activity of titanium dioxide samples for the dehydrogenation or oxidation of 2-propanol. Journal of Photochemistry and Photobiology A: Chemistry 59, 181–189.

Sclafani, A., Mozzanega, M.N., Herrmann, J.M., 1997. Influence of silver deposits on the photocatalytic activity of titania. Journal of Catalysis 168 (1), 117–120.

Seery, M.K., George, R., Floris, P., Pillai, S.C., 2007. Silver doped titanium dioxide nanomaterials for enhanced visible light photocatalysis. Journal of Photochemistry and Photobiology A: Chemistry 189, 258–263.

Sobsey, M.D., Fuji, T., Shields, P.A., 1988. Inactivation of hepatitis A virus and model viruses in water by free chlorine and monochloramine. Water Science and Technology 20 (11–12), 385–391.

Sommer, R., Pribil, W., Appelt, S., Gehringer, P., Eschweiler, H., Leth, H., Cabaj, A., Haider, T., 2001. Inactivation of bacteriophages in water by means of non-ionizing (UV-253. 7 nm) and ionizing (gamma) radiation: a comparative approach. Water Research 35 (13), 3109–3116.

Sordo, C., Van Grieken, R., Marugan, J., Fernandez-Ibanez, P., 2010. Solar photocatalytic disinfection with immobilised TiO_2 at pilot-plant scale. Water Science and Technology 61 (2), 507–512.

Stewart, S., Fredericks, P.M., 1999. Surface-enhanced Raman spectroscopy of peptides and proteins adsorbed on an electrochemically prepared silver surface. Spectrochimica Acta Part a-Molecular and Biomolecular Spectroscopy 55 (7–8), 1615–1640.

Sun, Y.F., Pignatello, J.J., 1995. Evidence for a surface dual hole – radical mechanism in the TiO_2 photocatalytic oxidation of 2,4-dichlorophenoxyacetic acid. Environmental Science & Technology 29 (8), 2065–2072.

Sung-Suh, H.M., Choi, J.R., Hah, H.J., Koo, S.M., Bae, Y.C., 2004. Comparison of Ag deposition effects on the photocatalytic activity of nanoparticulate TiO_2 under visible and UV light irradiation. Journal of Photochemistry and Photobiology A: Chemistry 163 (1–2), 37–44.

Tran, H., Scott, J., Chiang, K., Amal, A., 2006. Clarifying the role of silver deposits on titania for the photocatalytic mineralization of organic compounds. Journal of Photochemistry and Photobiology A: Chemistry 183, 41–52.

Tree, J.A., Adams, M.R., Lees, D.N., 2003. Chlorination of indicator bacteria and viruses in primary sewage effluent. Applied and Environmental Microbiology 69 (4), 2038–2043.

US Centers for Disease Control and Prevention, 2006. Surveillance for waterborne disease and outbreaks associated with drinking water and water not intended for drinking – United States, 2003–2004. Morbidity and Mortality Weekly Report Surveillance Summaries 55 (SS12), 31–58.

US Centers for Disease Control and Prevention, 2008. Surveillance for waterborne disease and outbreaks associated with drinking water and water not intended for drinking – United States, 2005–2006. Morbidity and Mortality Weekly Report Surveillance Summaries 57 (SS09), 39–62.

US Environmental Protection Agency, 2006a. National Primary Drinking Water Regulation: Long-Term 2 Enhanced Surface

Water Treatment Rule; Final Rule. Federal Register (40 CFR 9, 141, 142) 71:3, pp. 653–786.

US Environmental Protection Agency, 2006b. National Primary Drinking Water Regulations: Ground Water Rule; Final Rule. Federal Register (40 CFR 9, 141, 142) 71:216, pp. 65574–65659.

US Environmental Protection Agency, 2006c. National Primary Drinking Water Regulations: Stage 2 Disinfectants and Disinfection Byproducts Rule; Final Rule. Federal Register (40 CFR 9, 141, 142) 71:2, pp. 387–493.

Vamathevan, V., Amal, R., Beydoun, D., Low, G., McEvoy, S., 2002. Photocatalytic oxidation of organics in water using pure and silver-modified titanium dioxide particles. Journal of Photochemistry and Photobiology A: Chemistry 148 (1–3), 233–245.

Watts, R.J., Kong, S.H., Orr, M.P., Miller, G.C., Henry, B.E., 1995. Photocatalytic inactivation of coliform bacteria and viruses in secondary wastewater effluent. Water Research 29 (1), 95–100.

Wei, C., Lin, W.Y., Zainal, Z., Williams, N.E., Zhu, K., Kruzic, A.P., Smith, R.L., Rajeshwar, K., 1994. Bactericidal activity of TiO_2 photocatalysis in aqueous-media – towards a solar-assisted water disinfection system. Environmental Science & Technology 28 (5), 934–938.

Wong, M., Kumar, L., Jenkins, T.M., Xagoraraki, I., Phanikumar, M. S., Rose, J.B., 2009. Evaluation of public health risks at recreational beaches in Lake Michigan via detection of enteric viruses and a human-specific bacteriological marker. Water Research 43 (4), 1137–1149.

Xin, B.F., Jing, L.Q., Ren, Z.Y., Wang, B.Q., Fu, H.G., 2005. Effects of simultaneously doped and deposited Ag on the photocatalytic activity and surface states of TiO_2. Journal of Physical Chemistry B 109 (7), 2805–2809.

Yates, M.V., Malley, J., Rochelle, P., Hoffman, R., 2006. Effect of adenovirus resistance on UV disinfection requirements: a report on the state of adenovirus science. Journal-American Water Works Association 98 (6), 93–106.

Zhang, L.Z., Yu, J.C., Yip, H.Y., Li, Q., Kwong, K.W., Xu, A.W., Wong, P.K., 2003. Ambient light reduction strategy to synthesize silver nanoparticles and silver-coated TiO_2 with enhanced photocatalytic and bactericidal activities. Langmuir 19 (24), 10372–10380.